FURTHER APPLICATION OF BOMB ^{14}C AS A TRACER IN THE ATMOSPHERE AND OCEAN

REIDAR NYDAL and JORUNN S. GISLEFOSS

Radiological Dating Laboratory, The Norwegian Institute of Technology, N-7034 Trondheim NTH N-7034 Norway

ABSTRACT. Bomb ^{14}C from nuclear tests in the atmosphere has proved to be a particularly useful tool in the study of the carbon cycle. We provide here a *ca.* 30-yr time series of ^{14}C concentrations in the atmosphere between 28°N and 71°N and in the ocean surface between 45°S and 45°N. More recently (since 1990), a north-south profile also has been obtained for ^{14}C in the surface waters of the Atlantic Ocean. The measurements were performed using the conventional technique of beta counting of large samples (4 to 5 liter CO_2) in CO_2 proportional counters. These data show that the ^{14}C concentration in the atmosphere is leveling off with a time constant of 0.055 yr^{-1}, and is now approaching that of the ocean surface at lower latitudes.

Additional tracer studies have been concerned especially with the penetration of bomb ^{14}C into the deep ocean. The Norwegian and Greenland seas are of interest as a sink for atmospheric CO_2 and also a source of water for the deep Atlantic Ocean. During the last five years, several ^{14}C depth profiles have been measured from the Fram Strait (79°N) to south of Iceland (62°N), using the AMS technique available at the University of Arizona AMS Facility. We considered it important to repeat and compare a few of the profiles with those produced by the GEOSECS expedition in 1972 and the TTO expedition in 1981. The profiles show that water descending to the deep Atlantic Ocean is originating mainly from intermediate and surface depths in the Nordic Seas. However, the ventilation rate of the Norwegian Sea deepwater is too slow to be an important component in the transfer of water over the Greenland-Scotland Ridge.

INTRODUCTION

About 1000 nuclear tests, with a total strength of 500 MT (TNT equivalent), were carried out in the atmosphere from 1945 to 1962. About two-thirds of that energy was released at higher northern latitudes; mainly over Novaya Zemlya and mainly during the fall of 1961 and 1962 (UN Report 1964). The main atmospheric testing programs came to an end with the Test Ban Treaty of 5 August 1963 (The Moscow Treaty). France and China did not accept the Treaty immediately and continued to test smaller bombs in the atmosphere. France had its main testing period from 1966 to 1968 and carried these out in the Pacific Ocean. China carried out several tests over the Asian Continent (Lop Nor) until 1980, with the highest activity during the period 1968 to 1972. The total contribution from these post-1963 bomb tests was *ca.* 12% of the total power released into the atmosphere from nuclear testing.

We present here a further contribution to the carbon cycling research program, based on bomb ^{14}C as a tracer, which was initiated in our laboratory in 1962. From a noted doubling of the natural ^{14}C level at northern latitudes in 1962, the dispersion of bomb ^{14}C in the atmosphere and ocean surface has been studied extensively during subsequent years (Nydal and Løvseth 1983; Nydal *et al.* 1984). At present, the ^{14}C concentration in the atmosphere is approaching that of the ocean surface at lower latitudes. The tracing interest is now mainly concerned with the continuing penetration of bomb ^{14}C into the deep ocean. The arctic regions are especially in focus as they constitute sinks for atmospheric CO_2. Several cruises during recent years have been used to measure ^{14}C depth profiles in the Norwegian and Greenland Seas. These data are used to study the uptake of CO_2 in the Nordic Seas and its net transfer to the deepwater in the Atlantic Ocean (Nydal *et al.* 1991, 1992; Gislefoss *et al.* 1995).

SAMPLING AND MEASUREMENTS

The CO_2 sampling and conventional ^{14}C measurement of atmospheric CO_2 and ocean surface water are described in detail in earlier articles (Nydal and Løvseth 1983; Nydal *et al.* 1984). In brief sum-

mary: 1) sampling at ground level in the troposphere is performed with a solution of 1–2 liters NaOH (2%), which is exposed to the open air for several days. An absorption time of 7 days was generally applied from 1962–1981, but this was changed subsequently to 3–4 days. Depending on the air ventilation, between 3 and 6 liters of CO_2 are now absorbed over a period of 3 to 4 days; 2) sampling from the ocean surface is generally based on the recovery of 200 liters of seawater, collected at a depth of 5–10 m through the inlet of the pumping system of the ship. After acidifying the water (with H_3PO_4) to a pH value of *ca.* 3, a relative amount of between 4 and 6 liters of CO_2 is extracted in a flushing procedure on board the ship and absorbed in a bottle of 0.75 liters NaOH-solution (2%); 3) the conventional ^{14}C measurements were performed by beta counting 3–5 liters of CO_2 in proportional counters. The $^{14}C/^{13}C$ ratio is measured relative to the modern standard (NIST HOxII) and normalized for isotopic fractionation effects. The final ^{14}C enrichment for each sample is calculated and quoted in per mil excess above the pre-bomb level, according to the formula defined by Stuiver and Polach (1977)

$$\Delta^{14}C = \delta^{14}C - 2(\delta^{13}C + 25)\left(1 + \frac{\delta^{14}C}{1000}\right).$$ (1)

Until 1980, a counting time of 1–2 d per sample was used to ensure an analytical precision of *ca.* 10‰ (1 σ). After 1980, the counting time was increased to 4–5 days to obtain a better precision (4–5‰).

In earlier research from this laboratory, the $\Delta^{14}C$ values in the time series of bomb ^{14}C measurements were not corrected for radiometric decay of the modern reference standard, which is defined to equate AD 1950 with atmosphere. Compared to the earlier limit of error (up to 10‰) in those measurements, disregard for decay of the reference standard could be considered unimportant. However, after a decay period of 40 yr, the associated error of 5‰ is now comparable to the precision achieved in radiometric measurements. A retrospective correction for this decay has therefore been adopted for all our ^{14}C measurements, using the approximate correction formula

$$\Delta^{14}C_{corr} = \Delta^{14}C_{uncorr} + 1000[e^{\lambda(1950 - t)} - 1]$$ (2)

where λ is 1/8267 (5730 yr half-life) and *t* is the year of sampling. The corrected ^{14}C data are also available from the CDIAC database held at the Oak Ridge National Laboratory, Tennessee, USA.

The ^{14}C deep-sea profiles were initially achieved using large samples (100–200 liters seawater) and the radiometric ^{14}C counting technique. This collection procedure was very time-consuming. However, the recent availability of accelerator mass spectrometry (AMS) for ^{14}C measurement allows sampling to be based on much smaller water samples (0.5 liter). This technique brings exciting new possibilities for tracing ^{14}C in the deep sea (Gislefoss 1994; Gislefoss *et al.* 1994). The AMS measurements reported here were carried out at the NSF-Arizona AMS Laboratory in Tucson, Arizona. The procedure involves CO_2 samples between 1 and 2 ml being converted to CO over hot Zn, and further reduction of the CO to graphite over an iron catalyst at 625°C (Slota *et al.* 1987). The graphite powder is then pressed into an aluminum target holder for the AMS analysis. The $^{14}C/^{13}C$ isotope ratio of the sample graphite target is measured and compared to that recorded by the reference standards. An analytical precision of 4–5‰ is indicated by replicate analyses using independently prepared targets. Details of the experimental procedures are given by Linick *et al.* (1986) and associated calculations are quantified by Donahue, Linick and Jull (1990).

ATMOSPHERE

In the early 1960s, our program of ^{14}C measurements in the troposphere was set up based on CO_2 collected at a total of 14 stations sited between Madagascar (21°S, 47°E) and Svalbard (78°N, 13°E) (Nydal 1968; Nydal and Løvseth 1983). Over the years, it has not been possible to continue with this large number of stations, and from 1978 onward, the sampling network was reduced to two stations at Fruholmen, Nordkapp (71°06′N, 23°59′E; 70 m above sea level (asl)) and Izana, Tenerife (28°22′N, 16°03′E; 2400 m asl). The curve for Fruholmen is complete between 1963 and 1993. The curve measured at the Canary Islands is largely complete over the period 1963–1992, but comprises measurements from two neighboring stations; one at Izana, Tenerife and the other at Mas Palomas, Gran Canaria (27°45′N, 15°40′W; 10–100 m asl).
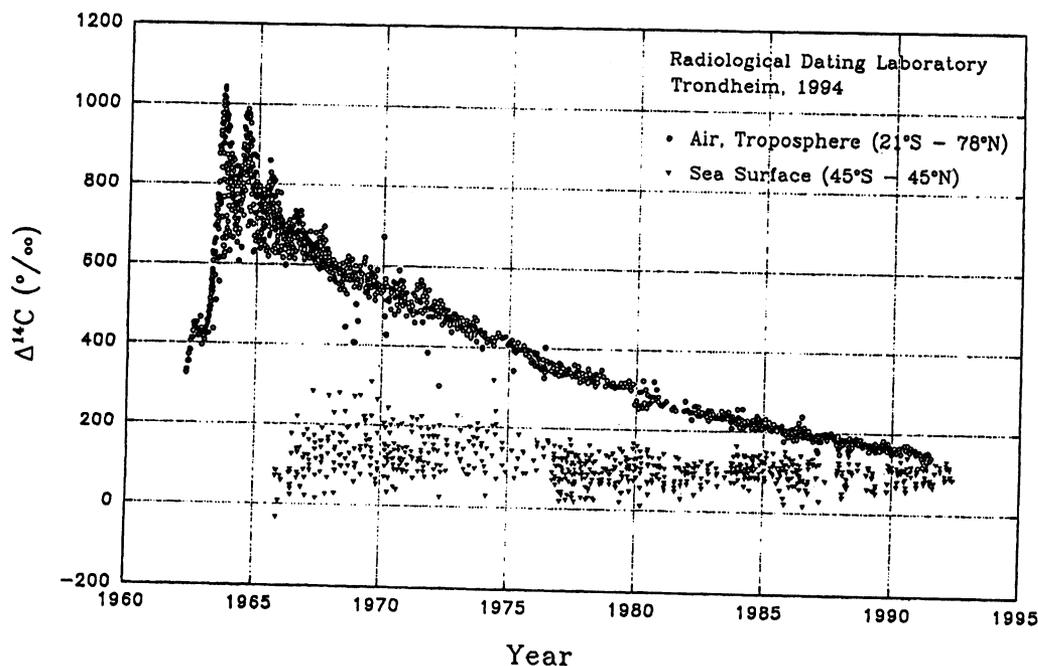

Fig. 1. ^{14}C in the troposphere and the ocean surface 1962–1992. Measurements only from Nordkapp (71°N) and Tenerife (28°N) after 1978.

A summary curve of the $\Delta^{14}C$ at all our tropospheric collection stations is given in Figure 1. The large seasonal variations in the troposphere values between 1963 and 1968 are caused mainly by the meteorological influx of ^{14}C from a concentration in the stratosphere 10 to 20 times higher during that early period (Feely, Katzman and Tucek 1966). The main exchange of CO_2 between the stratosphere and the troposphere occurs during the spring and summer, when the tropopause height increases toward higher latitudes. The magnitude of the seasonal variation in tropospheric ^{14}C concentration leveled off during the first years, until a further slight increase occurred from 1968 to 1972 as a result of French and Chinese tests. For subsequent years, the curve follows a more regular exponential decrease, with a decay constant of 0.055 yr^{-1}, calculated at Nordkapp from 1973 to 1992. Data in Figures 1 and 2 show that past AD 1980, there is a fairly close agreement between the curves recorded at Fruholmen (71°N) and Izana (28°N). Both collection stations enjoy relatively clean air and are within rapid circulation cells of the troposphere (Meijer *et al.* 1994).
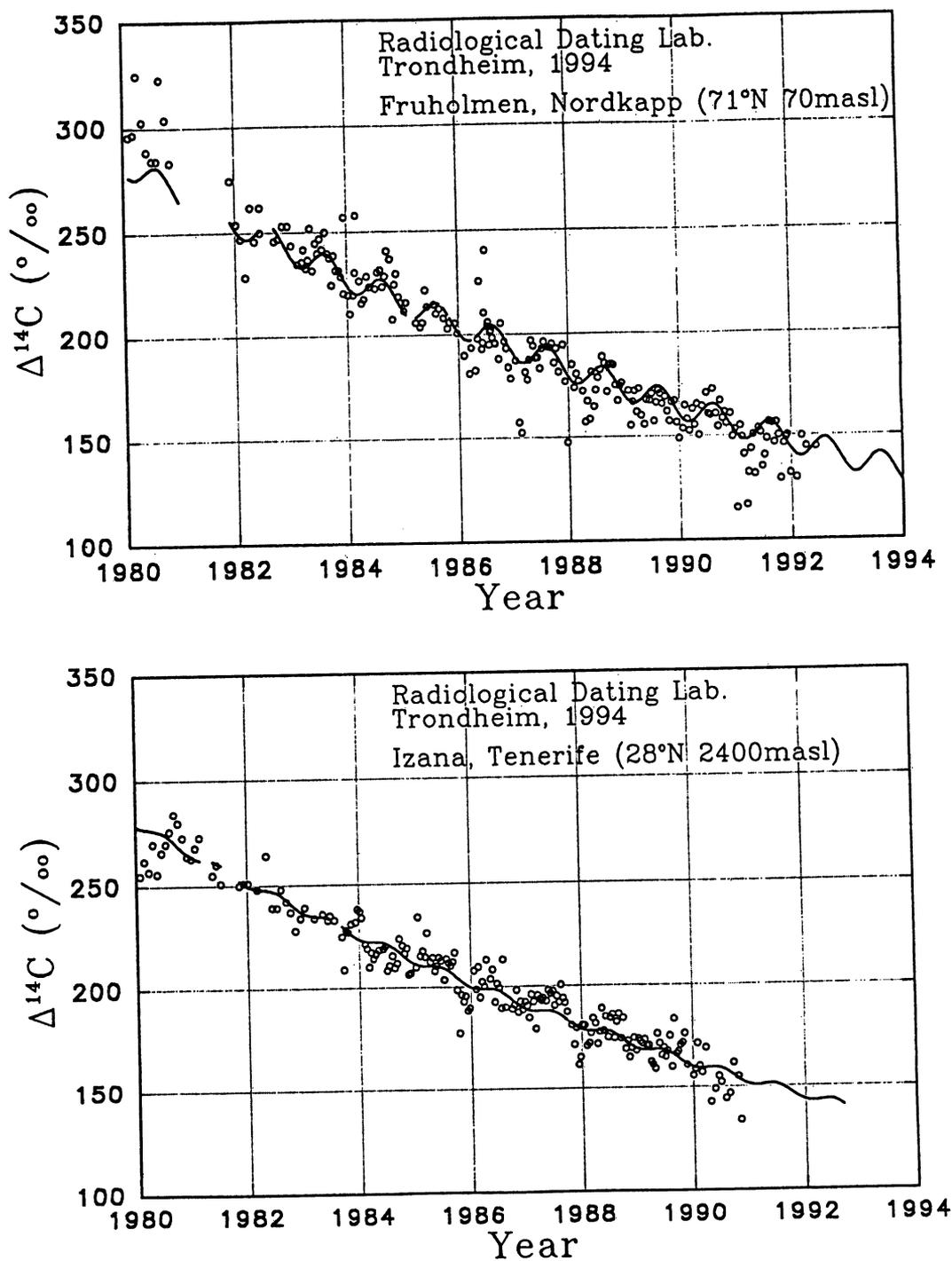
Fig. 2. 14C in the troposphere at Nordkapp (71°N) and Tenerife (28°N) 1980–1992

It is interesting to speculate on a possible signal in ^{14}C from the Chernobyl event of 26 April 1986. Two values of 30–40‰ above the ambient level at Fruholmen coincide with the time of this event (Fig. 1). Due to weather patterns prevalent at the time of the explosion, a low-pressure feature passing over Chernobyl subjected northern Scandinavian countries to radioactive fallout a few days later. Even though ^{14}C from the Chernobyl event can be regarded as negligible on a global scale, it is not surprising to find a more local and transient increase in this area.

Direct comparison of the temporal ^{14}C concentrations recorded from the two operational stations between 1980 and 1992 (Fig. 2) reveal seasonal variations with summer maxima and winter minima. The higher amplitude is found at Fruholmen, where the temporal variations are also more regular. A major cause of this pattern is dilution of $^{14}CO_2$ by the excess of inactive CO_2 (^{14}C-depleted) discharged to the atmosphere as a result of the greater combustion of fossil fuel during winter. This dilution effect levels off during the summer season, due to atmospheric mixing and ongoing exchange between the atmosphere and the other carbon reservoirs (ocean and biosphere). A comparison with ^{14}C concentrations recorded at sampling stations in central Europe (Levin *et al.* 1995) also indicates that seasonal variation is greater in areas with higher combustion of fossil fuel. A model simulation of the later (1980 to 1992) seasonal trend in the tropospheric ^{14}C concentrations recorded at Fruholmen and Izana has been attempted using the function

$$F(t) = A\sin 2\pi(t - t_o) + B\,e^{-k(t - t_o)} \quad. \tag{3}$$

The parameters A, B and t_o (Table 1) are determined *via* a least-square fit, whereas the decay constant k is calculated independently from a longer period at Fruholmen (1973 to 1992). To comply with the present observations in the ocean surface, and to avoid the spurious effect of additional parameters during a relatively short period, the ultimate level for the function was chosen to be zero. With an amplitude of 6.6 ± 1.4‰ and a decay constant of 0.055 yr^{-1}, the function gives the better fit to the Fruholmen, Nordkapp data. For the curve at Izana, Tenerife, the amplitude term (A) was reduced to approximately one-third of that used for Nordkapp. The seasonal variation and some of the ^{14}C data at Izana are more irregular than at Nordkapp, and do not always fit well with the calculated cycle. This latter observation reflects the special meteorological condition at Izana, as discussed previously (Nydal 1968).

TABLE 1. Parameters Obtained in a Least-Square Procedure (Marquardt-Levenberg Algorithm) for the Function (2) to fit the Data Sets from 1980 to 1992 from Nordkapp and Tenerife

Parameter	Parameter explanation	Nordkapp	Tenerife
A	Amplitude of the yearly oscillations	6.3 ± 1.3‰	1.9 ± 1.0‰
t_o	Time at the turning point of the cycle	1980.38 ± 0.03 yr	1980.25 ± 0.09 yr
B	The $\Delta^{14}C$ value at the time t_o	279.1 ± 1.2‰	276.6 ± 1.6‰
	Mean deviation from the curve	6.9%	7.3%

A small contribution to the seasonal variation of the ^{14}C in the troposphere could be from a still enhanced concentration of the $^{14}CO_2$ in the stratosphere. According to Tans (1981) the amount of bomb ^{14}C input to the stratosphere might have been underestimated significantly from sampling flights that took place after the cessation of nuclear testing. A few bombs tested in the upper atmosphere were significantly larger than the average and, in such instances, the induced radioactivity may have reached greater altitudes than expected. For example, a single hydrogen bomb over Novaya Zemlya on 30 October 1961 had a recorded 58 MT yield (SIPRI Yearbook 1975). Further-

more, a recently observed $\Delta^{14}C$ value of 250–275‰ at a height of 33–35 km (39.16°N, 141.83°E) by Nakamura *et al.* (1992) indicates a ^{14}C excess in the lower stratosphere that is still *ca.* 150‰ above the present tropospheric level. A progressively smaller part of this excess radioactivity will be transferred to the troposphere during spring and summer each year. However, according to the calculated residence time for ^{14}C in the upper stratosphere of 9.1 ± 0.2 yr, the present contribution from this source of bomb ^{14}C to the amplitude in the seasonal variation at ground level is <1‰.

OCEAN SURFACE

Prior to 1986, sampling of the ocean surface water was carried out from several ships crossing the Atlantic, Pacific and Indian Oceans (Nydal *et al.* 1984). During the last ten years, however, our sampling program has been restricted to a single ship of the Barber Line (MS *Tourcoing*), on its main global route from Europe, across the Atlantic Ocean to Panama, across the Pacific Ocean to New Zealand, northward to Japan and back across the North Pacific and Atlantic Oceans. In some cruises, the route to New Zealand has passed south through the Atlantic around the Cape of Good Hope to the Indian Ocean, with a return route through the Suez Canal and the Mediterranean Sea.

All of the ^{14}C measurements from ocean surface water that are shown in Figure 1 derive mainly from samples collected in the region 45°N to 45°S. The mean trend from all the scattered data approximates to a near-horizontal line at $\Delta^{14}C = 100$‰, which is close to the present atmospheric level. A closer study of ^{14}C in the surface ocean layer shows a pattern of seasonal variations that are normally correlated with ocean temperature. The largest variations coincide with upwelling areas along the continental margins, and the smallest variations are recorded in those stable parts of the open ocean least influenced by vertical mixing. Figure 3 shows the latitudinal variation of $\Delta^{14}C$ in the surface of the Atlantic Ocean from the pre-bomb level until present. The pre-bomb level is established from data compiled by Broecker and Peng (1982), and 1972–1973 data are reproduced from the GEOSECS expedition (Broecker *et al.* 1985). Our data were obtained with the Norwegian research vessel RV *Andenes* on a cruise to the Antarctic in the winter of 1989–1990 (Table 2) and are supplemented by more recent measurements (1990–1992) from the Nordic Seas (Table 3). These ^{14}C data concur reasonably well with the GEOSECS data reported for both sides of the Atlantic Ridge, and indicate that only small changes in $\Delta^{14}C$ have occurred in the ocean surface during the last 20 yr. It must be emphasized that the GEOSECS data show differences in magnitude between each side of the Ridge (Fig. 3, I and II) and therefore our more recent data have to be compared with the geographically closest GEOSECS values.

One of the main trends in the $\Delta^{14}C$ curves for the Atlantic Ocean is an approximate symmetry around the equator. The most stable surface layers (which exhibit the highest $\Delta^{14}C$ values) coincide with the high-pressure zones along both sides of the equator at about 30°N and 30°S. A slight decrease in $\Delta^{14}C$ occurs along the equator, where upwelling water with a lower ^{14}C concentration displaces the surface water toward higher latitudes (Broecker and Peng 1982). There is, however, a more dramatic lowering of ^{14}C enrichments towards higher latitudes, where the more stable surface layer vanishes. The Arctic Ocean (including Nordic Seas) behaves somewhat differently from the Antarctic, mainly due to the geographic distribution of the adjacent land areas. The Antarctic Ocean is unique in that total global circulation of the ocean currents is not impeded (Pickard and Emery 1990). Upwelling and downwelling of water both occur in this region (Foldvik and Gammelsrød 1988). The upwelling water displaces the surface layers and dilutes its ambient $\Delta^{14}C$ value.
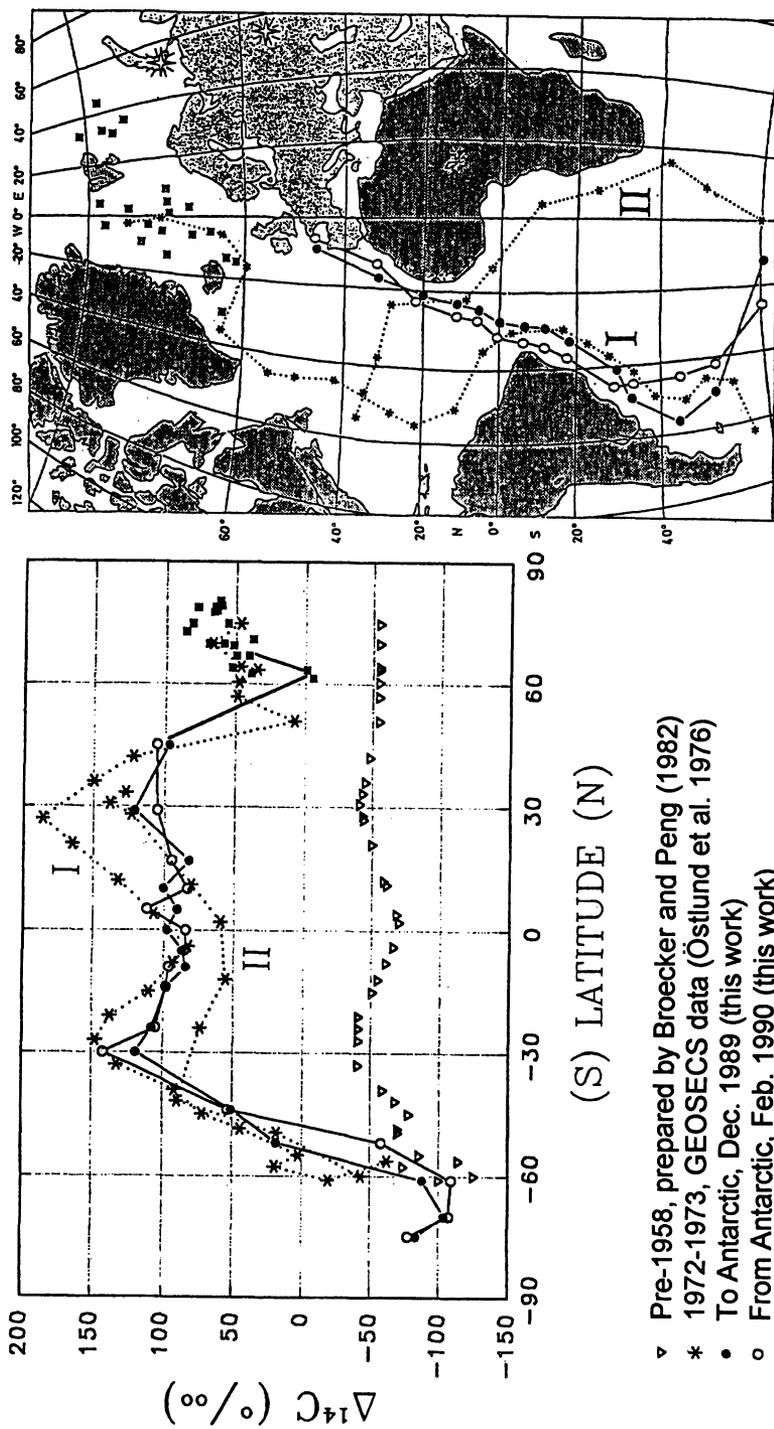
Fig. 3. A north-south profile of ^{14}C in the surface of the Atlantic Ocean 1989–1992

TABLE 2. [14]C Measurements in the Surface of the Atlantic Ocean from a Return Cruise to the Antarctic with RV *Andenes*, December 1989 to February 1990

Sample	Date (yy.mm.dd)	Location	$\delta^{14}C$ (‰)	$\delta^{13}C$ (‰)	$\Delta^{14}C$ (‰)
A-1	89.12.03	45°03′N 10°36′W	156	0.9	92.6 ± 5.7
A-2	89.12.08	29°34′N 20°00′W	181	0.5	117.2 ± 5.3
A-3	89.12.11	17°24′N 20°02′W	141	0.8	77.8 ± 4.1
A-4	89.12.12	10°00′N 22°21′W	161	1.5	96.1 ± 4.9
A-5	89.12.13	05°03′N 23°54′W	149	0.7	86.1 ± 4.4
A-6	89.12.14	00°24′N 25°41′W	157	0.9	93.6 ± 4.1
A-7	89.12.15	04°56′S 27°29′W	145	0.5	82.5 ± 4.3
A-8	89.12.16	09°46′S 29°00′W	143	1.2	79.5 ± 3.8
A-9	89.12.17	14°45′S 30°49′W	159	1.7	93.6 ± 3.9
A-10	89.12.21	24°34′S 37°48′W	171	1.8	104.0 ± 4.1
A-11	89.12.23	30°04′S 45°45′W	180	0.9	115.0 ± 4.2
A-12	89.12.30	44°37′S 56°14′W	111	2.3	46.5 ± 4
A-13	90.01.02	52°30′S 48°46′W	76	2.0	18.7 ± 4
A-14	90.01.08	61°42′S 14°12′W	−41	−0.6	−92.4 ± 3.8
A-15	90.01.16	70°03′S 12°35′W	−56	0.6	−108.4 ± 4.3
A-16	90.02.06	74°39′S 34°08′W	−37	−0.6	−88.1 ± 4.4
A-16(2)	90.02.09	73°58′S 33°01′W	−25	2.3	−82.2 ± 4.1
A-15(2)	90.02.16	70°03′S 12°35′W	−58	1.4	−111.4 ± 4.2
A-14(2)	90.02.25	59°54′S 28°12′W	−61	0.8	−113.3 ± 3.8
A-13(2)	90.02.28	52°19′S 37°03′W	−7	0.9	−62.6 ± 3.7
A-12(2)	90.03.01	44°58′S 38°47′W	111	2.8	49.2 ± 4.2
A-11(2)	90.03.05	30°23′S 41°36′W	185	1.2	118.9 ± 4
A-10(2)	90.03.06	25°00′S 42°41′W	168	1.7	101.4 ± 3.7
A-9(2)	90.03.13	13°26′S 34°28′W	161	2.4	93.9 ± 4.9
A-8(2)	90.03.14	09°38′S 32°44′W	157	1.6	91.7 ± 5.1
A-7(2)	90.03.15	05°04′S 30°34′W	146	2.0	80.5 ± 3.7
A-6(2)	90.03.16	00°25′S 28°29′W	146	1.9	80.1 ± 4.9
A-5(2)	90.03.17	04°50′N 26°08′W	154	1.5	89.1 ± 4.2
A-4(2)	90.03.19	10°09′N 23°50′W	143	1.1	79.0 ± 4.2
A-3(2)	90.03.20	16°39′N 20°56′W	136	1.6	71.6 ± 4.4
A-2(2)	90.03.24	30°13′N 14°40′W	165	0.9	100.8 ± 4.1
A-1(2)	90.03.27	44°36′N 08°51′W	164	0.2	101.6 ± 5

The southern limit of the Nordic Seas is determined by the shallow Greenland-Scotland Ridge, which serves to impede the exchange of water with the deep Atlantic Ocean. Toward the Atlantic Ocean there is very little upwelling, and sinking water generally is replaced from the Norwegian Atlantic and East Greenland surface currents. These features of the circulation pattern, together with a delay in downwelling caused by the shallow Greenland-Scotland Ridge, explains the fact that the present ^{14}C concentration in the surface water of the Nordic Seas exhibit a higher ^{14}C concentration ($\Delta^{14}C = +50$‰) than occurs at corresponding latitudes in the Antarctic Ocean ($\Delta^{14}C = -100$‰).

DEEP-SEA PROFILES IN THE NORDIC SEAS

During the last five years, our ^{14}C measurements of deep-sea profiles have been limited largely to the Nordic Seas, where the exchange processes are rapid enough to be studied within a limited period of time. The Greenland Sea is assumed to be one of the main source regions for deepwater

formed at higher latitudes (Smethie *et al.* 1986). The surface and intermediate waters sink as a result of surface cooling and deep convection during the winter. A mixture of deepwater from the Greenland Sea (GSDW) and the Eurasian basins (EBDW) is further assumed to be brought down through gaps in the ridge, to form the Norwegian Sea deepwater (NSDW) (Swift and Koltermann 1988; Bourke *et al.* 1993). An excess of water is also passing over the Greenland-Scotland Ridge to contribute to the deepwater in the Atlantic Ocean (AODW) (Swift *et al.* 1980). The locations of our ^{14}C profiles were chosen to give an optimal view of the transfer of carbon in this area (Fig. 4). The profiles are located in the East Greenland Current (A,C,E) at central positions in the main basins (D,F,G,I) in the Norwegian Atlantic Current and West Spitsbergen Current (B,H,J,K) and the Atlantic Ocean south of Iceland (L,M,N). The ^{14}C deep-sea profiles monitored 20 yr earlier during the GEOSECS expedition (Östlund, Dorsey and Brecher 1976), and some TTO profiles taken in 1981 (Östlund and Rooth 1981) have provided an important comparison and allowed a study based on changes that have occurred over that period.

TABLE 3. ^{14}C Measurements in the Surface of the Nordic Seas 1990–1992

Trondheim ref.	Arizona/ Trondheim (T)	Depth (m)	Date (yy.mm.dd)	Location	$\delta^{13}C$ (‰)	$\Delta^{14}C$ (‰)
LA1-1	T	4	90.07.21	77°43′N 32°30′E	--	61.5 ± 4.4
LA2-2A	T	50	90.07.23	78°12′N 29°50′E	--	59.4 ± 4.6
LA3-1	T	6	90.07.23	79°22′N 30°20′E	2.25	56.2 ± 4.2
LA4-1	T	5	90.07.27	79°01′N 41°54′E	2.28	60.3 ± 3.8
LA5-2A	T	5	90.07.30	80°31′N 29°12′E	--	57.0 ± 3.6
LA7-1	T	5	90.08.03	79°27′N 05°52′E	2.15	57.1 ± 4.6
LA8-2A	T	5	90.08.06	78°52′N 04°06′W	1.83	72.8 ± 6.1
LA10-01	T	6	90.08.11	74°59′N 02°29′W	1.54	51.3 ± 3.6
GS14-1	AA-7190	0	90.07.30	67°00′N 05°00′W	1.92	45.8 ± 4.0
GS14-2	AA-7191	10	90.07.30	67°00′N 05°00′W	1.84	37.1 ± 4.0
GS16-2	T	4	90.08.07	70°00′N 00°01′E	2.33	54.2 ± 3.8
GS17-2	T	5	90.08.10	69°31′N 14°50′W	--	47.3 ± 4.0
GS18-1B	T	4	90.08.11	71°08′N 07°29′W	--	33.1 ± 4.5
GS19-1A	T	4	90.08.13	69°57′N 09°36′E	--	65.1 ± 3.7
LA15-2	AA-8730	10	91.08.16	74°59′N 11°31′W	1.44	77.5 ± 4.7
MO16-1	AA-11940	4.5	91.09.06	62°35′N 15°31′W	2.32	35.4 ± 4.3
JH5-212	AA-9871	3	92.07.15	64°00′N 04°60′W	1.85	49.2 ± 4.1
JH9-212	AA-10203	5	92.07.16	61°31′N 16°20′W	0.98	−9.2 ± 4.2
JH10-212	AA-10139	4	92.07.19	63°30′N 32°30′W	1.69	−4.4 ± 4.7

The cyclonic Greenland gyre is supported by the West Spitsbergen Current in the east and the East Greenland Current in the west. It is constrained between the Fram Strait in the north and the Norwegian Sea in the south. Four deep-sea profiles of $\Delta^{14}C$ were obtained in this area (A,B,C,D, in Fig. 5a). Profiles A and B show typical differences in water masses and exchange on each side of the Fram Strait.[1] The East Greenland Current profile (LA8, LA17) shows a linear gradient from the surface to a depth of 1000 m. Between 1000- and 2000-m depth, the curve is more irregular and certainly due to the influence of other water masses. This deeper part of the profile also has a slightly higher salinity than in the middle of the Greenland Sea (Nydal *et al.* 1991) and probably reflects the influence of the saltier EBDW. The apparent $\Delta^{14}C$ inversion between *ca.* 1200- and 1800-m depth also indicates the influence of water from the relatively young GSDW.

[1]Note that the alphabetic indices in Figure 4 correspond to the profiles shown in Figure 5a, b, c and d.
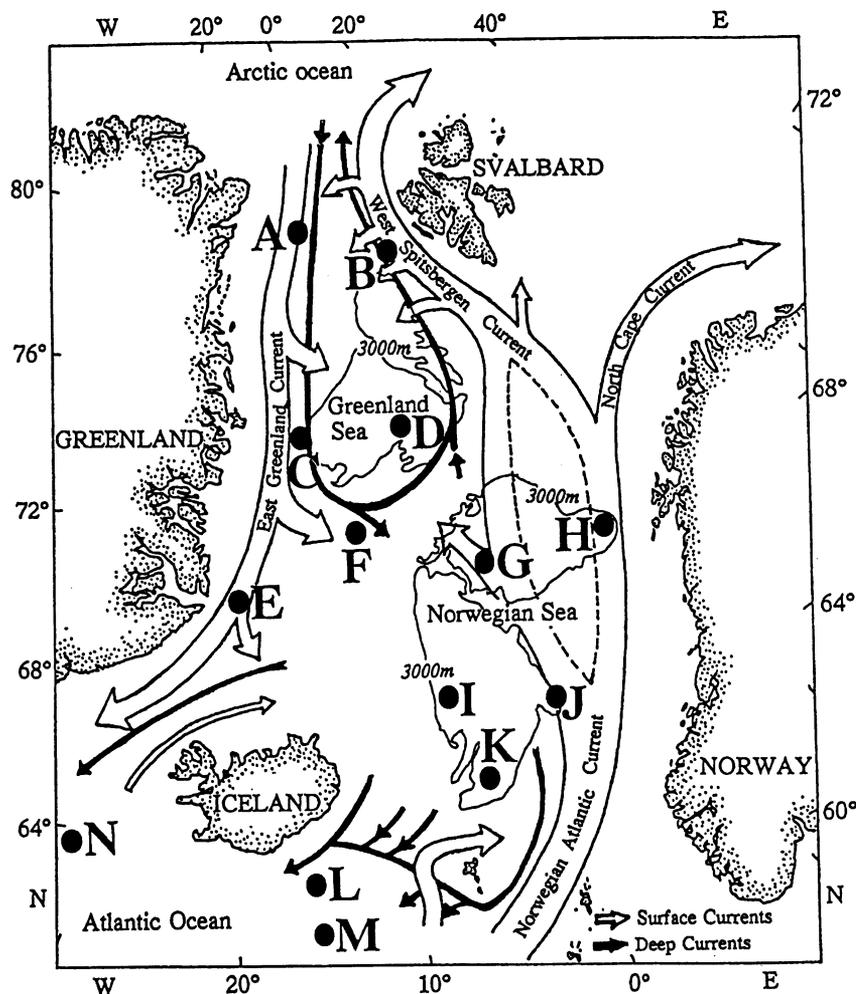
Fig. 4. Map of ^{14}C depth profiles in the Nordic Seas 1989–1992. The various letters A, B,…N indicate the approximate locations of the ^{14}C profiles seen in Fig. 5a,b,c,d.

The West Spitsbergen Current is a branch of the salty and warm Norwegian Atlantic Current. This is reflected in the $\Delta^{14}C$ values of the upper *ca.* 500 m of profile B (LA7), which records a small vertical gradient. The steepest gradient for vertical exchange occurs between 500 and 1000 m, where the $\Delta^{14}C$ values change by *ca.* 100‰. There is a further small decrease in $\Delta^{14}C$ down to 2000 m depth. The few neighboring TTO data from 1981 (Sta. 154 and 156) were collected closer to Svalbard, but they seem to support the shape of our profile.

Profile C (LA15), taken in the East Greenland Current, has a similar pattern to profile A. However, in this location, the linear trend extends to a depth below 2000 m. The curve is supplemented by three measurements from greater depth, taken just outside the shelf (LA14), which seem to fit well with the deepwater data for the northern profile (A). This feature indicates that the younger GSDW is affecting the profile at greater depth, *i.e., ca.* 2000–3000 m. The decrease in the ^{14}C concentrations below 3000 m suggests the influence of a deep current that may be connected to the NSDW.

In Profile D, data collected in the center of the Greenland gyre (LA10) are compared to the earlier GEOSECS (Sta. 17) and TTO (Sta. 148) profiles collected 18 and 9 yr earlier at approximately the same location. LA10 shows a $\Delta^{14}C$ range between +50‰ in the ocean surface to a mean value of –39 ± 2‰ (4 samples) below 2000 m depth. The lack of a $\Delta^{14}C$ depth gradient between 2000 and *ca.* 3500 m may indicate a well-mixed deep reservoir with a rapid internal circulation. We calculate that $\Delta^{14}C$ values in the deepest part of the profile have increased by 12 ± 2‰ relative to the GEOSECS profile recorded in 1972. An extrapolation back to the pre-bomb level (*ca.* 1960) in the deepwater is difficult to perform, because of little data and later change in deepwater formation (Schlosser *et al.* 1991). A linear increase in the sequestration rate of the tracer indicates, however, a pre-bomb $\Delta^{14}C$ level of *ca.* –60‰ for GDSW, a value close to that obtained for the surface water. The $\Delta^{14}C$ value of –59 ± 3‰ in the surface water is based on measurements of marine shells from Northern Norway and Spitsbergen (Mangerud and Gulliksen 1975). All of the TTO data from 1981 have $\Delta^{14}C$ values intermediate between the GEOSECS data and our 1990 values.

The area immediately south of the Greenland Sea, designated as the Norwegian and Icelandic Seas, is covered by four profiles (E,F,G,H; Fig. 5b), taken at virtually the same latitude, *i.e.*, 69° to 71°N. The upper parts of these profiles show a gradual change from the East Greenland Current (E) to the Lofoten Basin (H). Profile E, which includes two neighboring stations (GS17 and MO14), records a linear decrease in ^{14}C concentration from the surface to *ca.* 1500-m depth. The other profiles show a gradual eastward influence from the Norwegian Atlantic Current in the tendency to more uniform $\Delta^{14}C$ values in their upper depth ranges.

In Profile F (GS18), our measurements are compared with the TTO profile (Sta. 159) taken in 1981 at a slightly different location. If we assume that the two sampling locations represent the same water mass, then the comparison shows that the $\Delta^{14}C$ value below 500 m has increased by 15–20‰ between 1981 and 1990.

In Profile G (GS16), our measurements are compared with the GEOSECS (Sta. 18) and the TTO (Sta. 144) profiles. The earlier profiles show no significant input of bomb ^{14}C below 2000 m depth between 1972 and 1981. An increase of 7–8‰ was observed, however, in 1990. This is taken to indicate that the deep convection only reached this deepwater between 1981 and 1990. Compared to Profile D taken in the central Greenland Sea, the deepwater at location G is older and more in agreement with the water found at 2000 m depth in the periphery of the Greenland Gyre (C).

Farther south and into the more central part of the Norwegian Sea (Fig. 5c), we find that the deepwater becomes progressively older still. A comparison of the time-transient data in Profile I (GS14, MO10, GEOSECS (Sta. 19) and TTO (Sta. 144)) shows no significant differences in $\Delta^{14}C$ for water collected below 2000 m. The mean $\Delta^{14}C$ value of –73 ± 3‰ (6 samples) from the 1990–1991 measurements should not be much different from the pre-bomb level. The pre-bomb $\Delta^{14}C$ value in the NSDW is at least 10‰ lower than that of the surface water of the Greenland Sea. This corresponds to a decay of ^{14}C during a period of 100 yr from the surface to the deep Norwegian Sea. If the NSDW was mainly fed from the Greenland Sea, this period should be identical with the mean age of the NSDW. This water is, however, also in exchange with the EBDW, with other $\Delta^{14}C$ values that may modify the calculated age of the NSDW (Bønisch and Schlosser 1995).

The two profiles (J,K, Fig. 5c) measured in the southern Norwegian Sea indicate that the vertical mixing is faster at the periphery of the basin than in the central part. This is demonstrated clearly in Profile K, where our data (JH5) can be compared directly with that recorded at the GEOSECS station (19) in 1972. The other Profile J (weather ship station) over the slope of the Norwegian shelf is our only winter profile in the Nordic Seas. This profile has an identical pattern to a depth of *ca.*
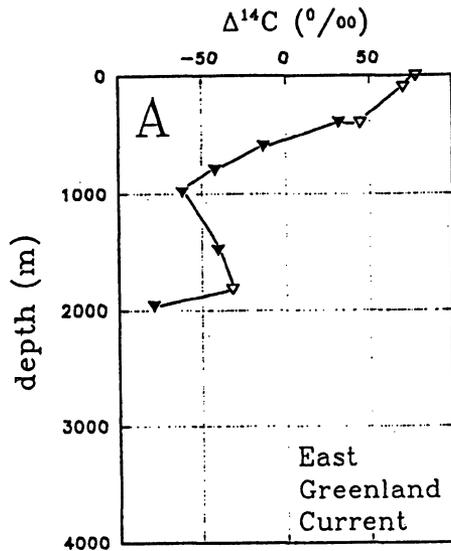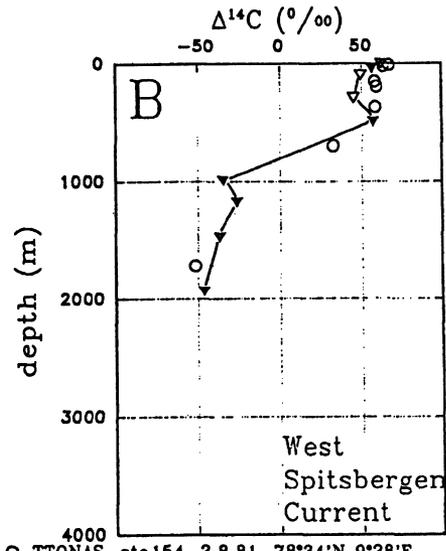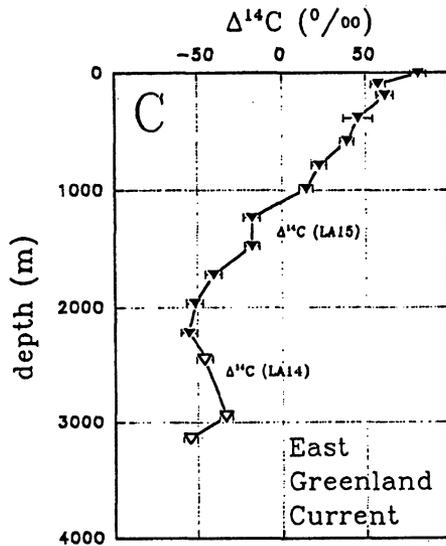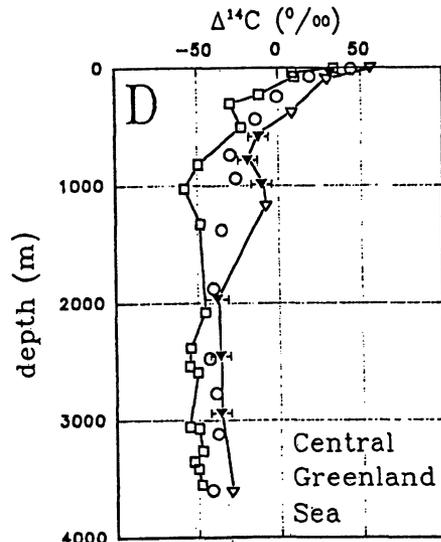
Fig. 5a. ¹⁴C depth profiles in the Greenland Sea
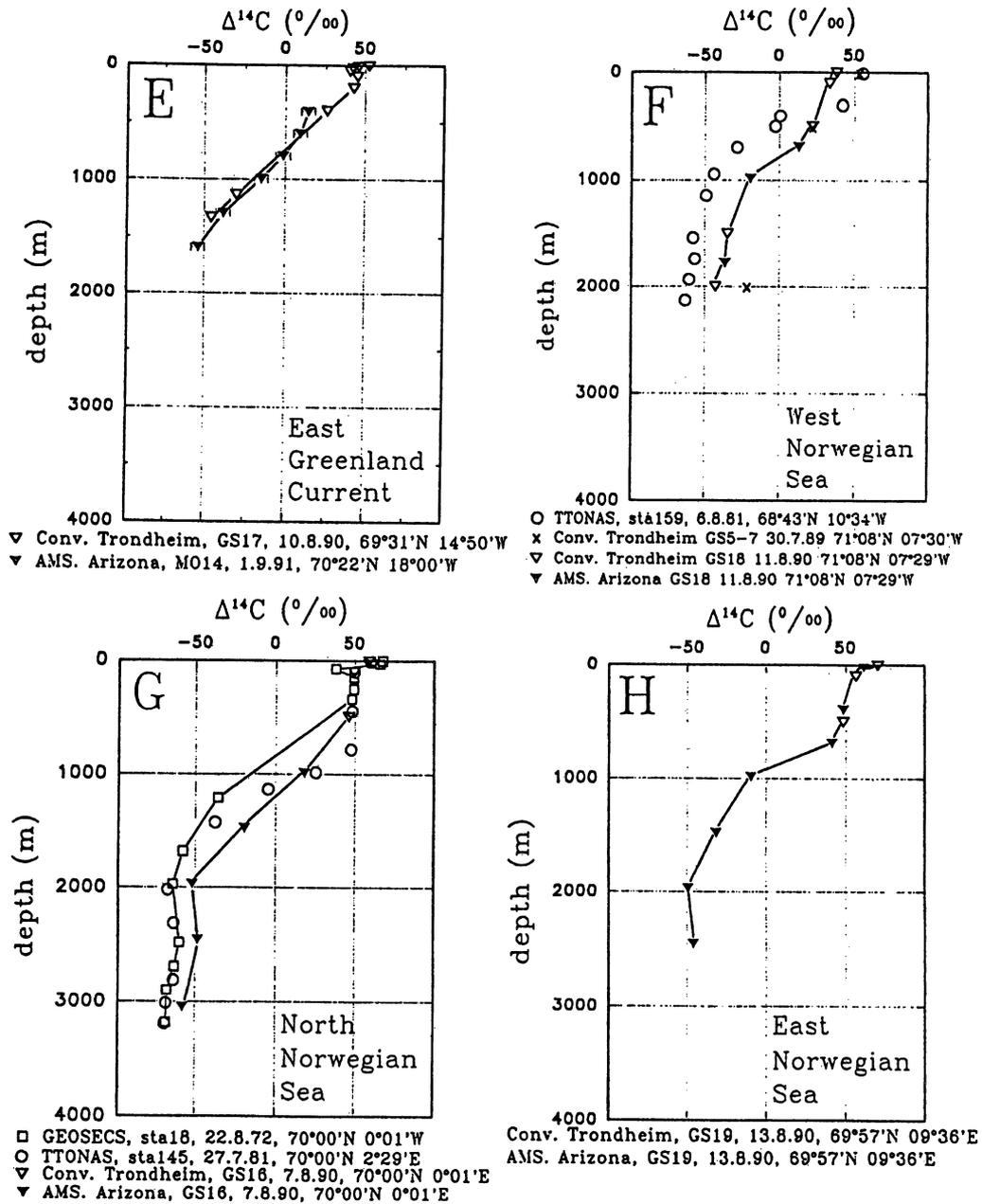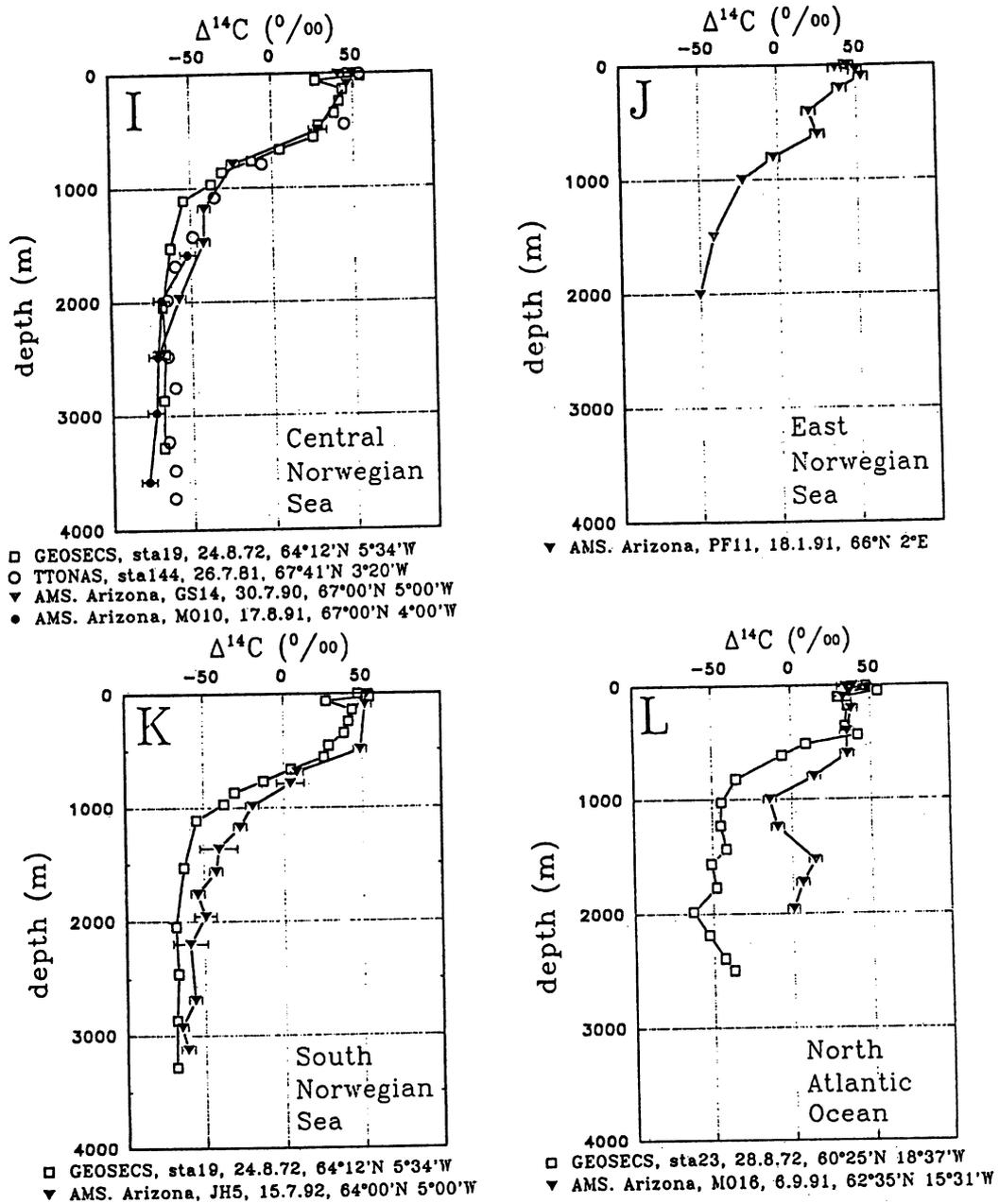
Fig. 5c. ^{14}C depth profiles from the Norwegian Sea to south of Iceland

2000 m where the recorded $\Delta^{14}C$ value is *ca.* −50‰. A similar value is recorded in all the profiles (B,H,J,K) taken along the shelf.

The most important changes in the ^{14}C depth profiles appear across the ridge and down to the North Atlantic Ocean. In profiles L (MO16) and M (JH9) our data are compared with the GEOSECS profile (Sta. 23) 1–2° further south; JH9 is also compared with the TTO profile (Sta. 142) some 8° further east (Fig. 5c,d). The two recent profiles, which are slightly apart, have the same trend as the GEOSECS profile. The comparison shows that a rapid downwelling occurs south of the ridge. The $\Delta^{14}C$ value below 1000 m is variable between +10 and −10‰, and this feature indicates that the NSDW makes a very small contribution to the overflow of water into the formation of the AODW. The downwelling water consists of mainly surface- and intermediate water, a result which is in accordance with that earlier pointed out by Heinze *et al.* (1990). The TTO profile from 1981 represents shallower water collected on the ridge further east.

Profile N, for the North Atlantic Ocean, compares our recent data (JH10) with the GEOSECS record (Sta. 11) obtained 3° further west (below the Denmark Strait) in 1972, and five TTO stations (164, 169, 170, 171) in the same general area sampled in 1981. The deepwater reflects surface and intermediate water from north of the ridge, in agreement with Strass *et al.* (1993) The TTO and GEOSECS profiles agree fairly well, but show a marked deviation from our profile (JH10). This raises the question as to whether this is caused by an unknown accident in sample treatment at this location, or by a temporary aberration due to local circumstances. During a later cruise (Nordic WOCE 1994) we were not able to reproduce this curve, but obtained data more in agreement with the TTO result.


□ GEOSECS, sta23, 28.8.72, 60°25'N 18°37'W
○ TTONAS, sta142, 24.7.81, 61°20'N 8°01'W
▼ AMS. Arizona, JH9, 16.7.92 61°31'N 16°20'W

□ GEOSECS, sta11, 5.8.72, 63°32'N 35°14'W
○ TTONAS, sta164, 11.8.81, 62°30'N 30°24'W
▽ TTONAS, sta167, 13.8.81, 64°5'N 33°19'W
△ TTONAS, sta169, 13.8.81, 64°39'N 34°5'W
◇ TTONAS, sta170, 14.8.81, 65°6'N 34°31'W
✳ TTONAS, sta171, 14.8.81, 63°40'N 33°19'W
▼ AMS. Arizona, JH10, 19.7.92 63°30'N 32°30'W
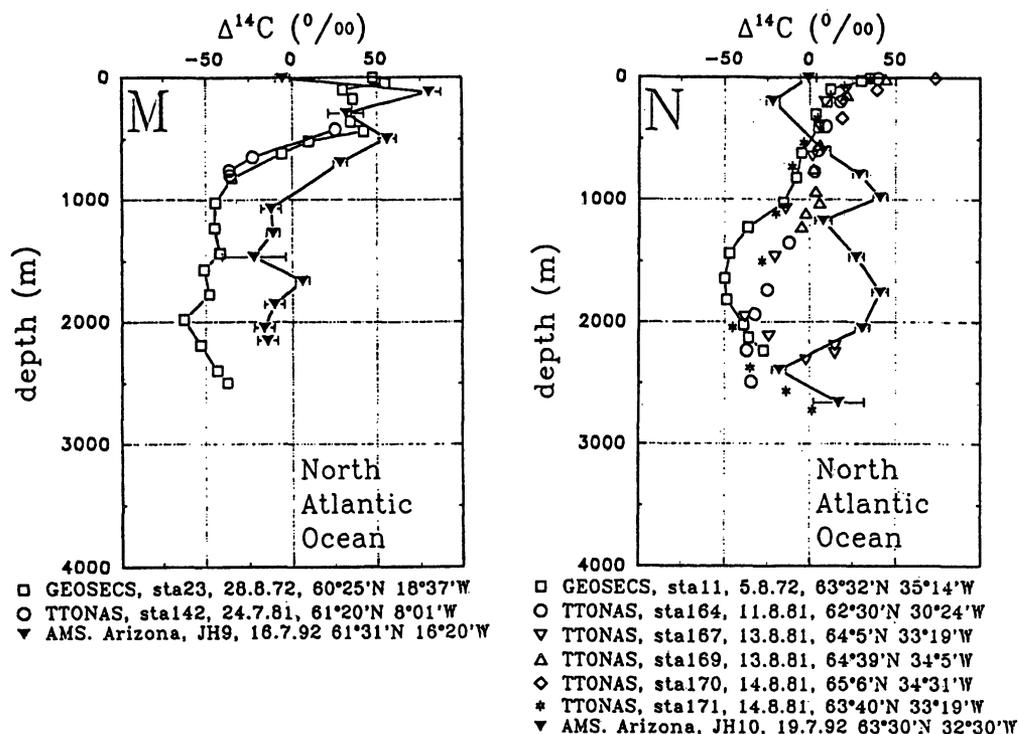
Fig. 5d. ^{14}C depth profiles in the Atlantic Ocean south of Iceland

SUMMARY AND CONCLUSION

In addition to those progressive changes recorded in the concentration of CO_2 in the atmosphere, the time-dependent distribution pattern for "bomb [14]C" introduced into the upper atmosphere during nuclear weapons test programs is an important tool for testing models that describe carbon exchange in nature. Here we have presented and discussed several such ^{14}C data sets recorded *via* samples collected over the past 30 yr from the lower atmosphere (troposphere) and oceans.

The trend in atmospheric ^{14}C concentrations recorded from northern Norway and the Canary Islands show large seasonal variations during the 1960s due to the net downward transfer of the major excess of "bomb [14]C" that had been injected directly into the stratosphere. Both curves indicate that, after 1972, the troposphere can be considered in general as a single well-mixed reservoir of "bomb [14]C", but with some very small localized disturbances still evident. Both sampling stations record an almost exponential decrease in the concentration of excess ^{14}C, with a rate constant of 0.055 yr^{-1}. Where small seasonal variations still occur, these are in the main due to localized dilution by ^{14}C-free CO_2 produced by the increased combustion of fossil fuels in winter. By 1992, the Δ^{14}C level in the lower atmosphere was *ca.* +100‰ above the pre-bomb level, and this was equal to the ^{14}C enrichment recorded in surface ocean water at equatorial latitudes (45°N to 45°S).

For the past 25 yr, the trend in Δ^{14}C in the equatorial surface ocean can be approximated by a horizontal line, *i.e.,* no significant temporal variation has occurred during that time. This feature reflects the role of the water mass as an effective buffer to ^{14}C exchange between the atmosphere and the intermediate and deep ocean carbon reservoirs. The Δ^{14}C profile of Atlantic Ocean surface water shows an approximate latitudinal symmetry around the equator poleward to 60°N/S, with the most stable regions coincident with the atmospheric high pressure cells at 30°N and 30°S. A slight decrease in ^{14}C concentration occurs at the equator, but a more dramatic lowering is evident toward higher latitudes, where the more stable surface layer vanishes.

The rate of further decrease in the amount of "bomb [14]C" in the atmosphere will be governed mainly by the ongoing exchange of CO_2 with the deep ocean. For the past five years, we have attempted to use ^{14}C as a tracer to study the transfer of carbon from the Nordic Seas to the deepwater reservoir of the Atlantic Ocean. Several deep-sea profiles have been produced to cover the North Atlantic Ocean from south of Iceland northward to the Fram Strait. These data have been compared with similar profiles obtained during the GEOSECS expedition in 1972 and the TTO expedition in 1981. Our measurements confirm that the water that is moving southward over the Greenland-Scotland Ridge into the deep Atlantic derives mainly from surface and intermediate depths in the Nordic Seas. The deepwater in the central region of the Norwegian Sea is too dense to have an important role in the mass transfer over the ridge. The obtained age of the NSDW is *ca.* 100 yr in the case that the main water derives from the surface of the Greenland Sea. The additional exchange of water between the NSDW and the EBDW may, however, modify this result.

REFERENCES

Bønisch, G. and Schlosser, P. 1995 Deep water formation and exchange rates in the Greenland/Norwegian Seas and the Eurasian Basin of the Arctic Ocean as derived from tracer balances. *Progress in Oceanography* 35: 29–52.

Bourke, R. H., Paquette, R. G., Blythe, R. F. and Stone, M. D. 1993 On the deep and bottom waters of the Greenland Sea from summer 1989 to 1990 data. *Journal of Geophysical Research* 98(C3): 4629–4638.

Broecker, W. S. and Peng, T.-H. 1982 *Tracers in the Sea.* Palisades, New York, Eldigio Press: 690 p.

Broecker, W. S., Peng, T.-H., Östlund, G. and Stuiver, M. 1985 The distribution of bomb radiocarbon in the ocean. *Journal of Geophysical Research* 90(C4): 6953–6970.

Donahue, D. J., Linick, T. W. and Jull, A. J. T. 1990 Isotope-ratio and background corrections for accelerator mass spectrometry radiocarbon measurements. *Radiocarbon* 32(2): 135–142.

Feely, H. W., Katzman, D. and Tucek, C. S. 1966 16th Progress Report Project Stardust, DASA.

Foldvik, A. and Gammelsrød, T. 1988 Notes on southern ocean hydrography, sea-ice and bottom water formation. *Paleogeography, Paleoclimatology and Paleoecology* 67: 3–17.

Gislefoss, J. S. 1994 Carbon profiles in the Nordic Seas. PhD. dissertation, NTH-Trondheim: 170 p.

Gislefoss, J., Nydal, R., Donahue, D. J., Jull, A. J. T. and Toolin, L. J. 1994 Tracer studies of ^{14}C in the Nordic Seas by AMS measurements. *Nuclear Instruments and Methods in Physics Research* B92: 431–435.

Gislefoss, J. S., Nydal, R., Skjelvan, I., Nes, A., Østerhus, S., Holmén, K., Jull, T. and Sonninen, E. 1995 Carbon profiles in the Nordic Seas. *Data Report* 2. Radiological Dating Laboratory, Trondheim, Tapir: 61 p.

Heinze, C., Schlosser, P., Koltermann, K. P. and Meincke, J. 1990 A tracer study of the deep water renewal in the European polar seas. *Deep-Sea Research* 37(9): 1425–1453.

Levin, I., Graul, R. and Trivett, N. B. A. 1995 Long-term observations of atmospheric CO_2 and carbon isotopes at continental sites in Germany. *Tellus* 47B (Series B): 23–34.

Linick, T. W., Jull, A. J. T., Toolin, L. J. and Donahue, D. J. 1986 Operation of the NSF-Arizona Desolator Facility for Radioisotope Analysis and results from selected collaborative research projects. *In* Stuiver, M. and Kra, R. S., eds., Proceedings of the 12th International ^{14}C Conference. *Radiocarbon* 28(2A): 522–533.

Mangerud, J. and Gulliksen, S. 1975 Apparent radiocarbon ages of recent marine shells from Norway, Spitsbergen and Arctic Canada. *Quaternary Research* 5: 263–273.

Meijer, H. A. J., van der Plicht, J., Gislefoss, J. S. and Nydal, R. 1994 Comparing long-term atmospheric ^{14}C and ^{3}H records near Groningen, The Netherlands with Fruholmen, Norway and Izaña, Canary Islands. *Radiocarbon* 37(1): 39–50.

Nakamura, T., Nakazawa, T., Nakai, N., Kitagawa, H.,

Honda, H., Itoh, T., Machida, T. and Matsumoto, E. 1992 Measurement of ^{14}C concentrations of stratospheric CO_2 by accelerator mass spectrometry. *In* Long, A. and Kra, R. S., eds., Proceedings of the 14th International ^{14}C Conference. *Radiocarbon* 34(2): 745–752.

Nydal, R. 1968 Further investigation on the transfer of radiocarbon in nature. *Journal of Geophysical Research* 73(12): 3617–3635.

Nydal, R. 1993 Application of bomb ^{14}C as a tracer in the global carbon cycle. *Trends in Geophysical Research* 2: 355–364.

Nydal, R., Gislefoss, J., Skjelvan, I., Blindheim, J., Foldvik, A., Vinje, T. and Østerhus, S. 1991 Measurements of carbon profiles in the Nordic seas. *Norsk Polarinstitutt Rapportserie, Datareport* 75: 1–43.

Nydal, R., Gislefoss, J., Skjelvan, I., Skogseth, F. H., Jull, A. J. T. and Donahue, D. J. 1992 ^{14}C profiles in the Norwegian and Greenland Seas by conventional AMS measurements. *In* Long, A. and Kra, R. S., eds., Proceedings of the 14th International ^{14}C Conference. *Radiocarbon* 34(3): 717–726.

Nydal, R., Gulliksen, S., Løvseth, K. and Skogseth, F. H. 1984 Bomb ^{14}C in the ocean surface, 1966–1981. *Radiocarbon* 26(1): 7–45.

Nydal, R. and Løvseth, K. 1983 Tracing bomb ^{14}C in the atmosphere 1962–1980. *Journal of Geophysical Research* 88(C6): 3621–3635.

Östlund, H. G., Dorsey, H. G. and Brecher, R. (ms.) 1976 GEOSECS Atlantic, radiocarbon and tritium results. Data report from Rosenstiel School of Marine and Atmospheric Sciences. Florida, University of Miami: 93 p.

Östlund, H. G. and Rooth, C. G. H. 1990 The North Atlantic tritium and radiocarbon transients 1972–1983. *Journal of Geophysical Research* 95(C11): 20,147–20,165.

Pickard, G. L. and Emery, W. J. 1990 *Descriptive Physical Oceanography.* Oxford, Pergamon Press: 320 p.

Schlosser, P., Bönisch, G., Rhein, M. and Bayer, R. 1991 Reduction of deep-water formation in the Greenland Sea during the 1980s: Evidence from tracer data. *Science* 251: 1054–1056.

SIPRI Yearbook 1975 *World Armament and Disarmaments.* Stockholm, Almqvist & Wiksell.

Slota, P. J., Jr., Jull, A. J. T., Linick, T. W. and Toolin, L. J. 1987 Preparation of small samples for ^{14}C accelerator targets by catalytic reduction of CO. *Radiocarbon* 29(2): 303–306.

Smethie, W. M., Jr., Östlund, H. G., and Loosli, H. H. 1986 Ventilation of the deep Greenland and Norwegian seas: Evidence from krypton-85, tritium, carbon-14 and argon-39. *Deep-Sea Research* 33: 675–703.

Strass, V. H., Fairbach, E., Schauer, U. and Sellmann, L. 1993 Formation of Denmark Strait overflow water by missing the East Greenland Current. *Journal of Geophysical Research* 90(C4): 6907–6919.

Stuiver, M. and Polach, H. A. 1977 Discussion: Reporting of ^{14}C data. *Radiocarbon* 19(3): 355–363.

Swift, J. H., Aagaard, K. and Malmberg, S.-A. 1980 The contribution of the Denmark Strait overflow to the deep North Atlantic. *Deep-Sea Research* 27A: 29–42.

Swift, J. H. and Koltermann, K. P. 1988 The origin of Norwegian Sea deep water. *Journal of Geophysical Research* 93: 3563–3569.

Tans, P. 1981 A compilation of bomb ^{14}C data for use in global carbon model calculation. *In* Bolin, B., ed., *Carbon Cycle Modeling.* SCOPE: 390 p.

U.N. Report 1964 Radioactive contamination of the environment by nuclear tests, effect of atomic radiation. *United Nations Scientific Committee Report* 14 (A/5814): 120 p.